acetic acid was carried out for 30 min at 60°C. The solutions of distilled water and 4% acetic acid were analysed by LC/ED. In contrast, the migration test into *n*-heptane was carried out for 60 min at 25°C and 5 ml of the *n*-heptane solution obtained was evaporated to dryness using a rotary evaporator. The samples were redissolved in 5 ml of methanol, and determined by LC/ED. Migration levels of NP were calculated by the ratio of volume to film area. A 100 cm^2 piece of the film was cut using a template and immersed in 10.0 ml of pre-heated solvents. These food simulant solvents and the following conditions are as stipulated in Japanese regulations. This condition was adapted for this purpose because this is simple and useful.

Exposure of PVC films to food

The issue of whether NP contained in the PVC films is released into food, requires migration levels of NP into food to be determined. It is reasonable to test this potential for migration using rice as a model food.

Recovery tests of NP added to cooked rice samples were performed by extraction with acetonitrile using only glassware. A rice sample (10 mg) was spiked with a solution of 100 µg/ml (sample concentration of 100 ng/g). Extraction of NP was carried out with acetonitrile (30 ml) added to 10 mg of the rice sample and sonicated for 10 min. The acetonitrile solution was then collected in a flask. The rice sample was re-extracted three times with acetonitrile (30 ml) in the same manner. *n*-Hexane saturated with acetonitrile (30 ml) was added to the mixture, followed by vigorous shaking in a separating funnel. The acetonitrile phase was collected in a 200 ml round-bottomed flask and evaporated to dryness with a rotary evaporator. The samples were redissolved in 10 ml of methanol.

Determination of NP levels in food (cooked rice) wrapped in PVC film was carried out as above. The cooked rice was allowed to cool to room temperature for 10 min. The rice sample (10 g) was wrapped completely in PVC film. The mass of the PVC film was 4 g and 90 cm^2 of film was in contact with the 10 g rice sample. This sample wrapped in PVC film was exposed in two ways. In the first the sample was reheated in a microwave oven (500 W, 2450 MHz) for 1 min. In the second, the sample was kept for 30 min at room temperature. Subsequent extraction employed acetonitrile, as described above. Samples (10 mg) were taken from the outside, which was in contact with the PVC film, and the inside, where there was no direct contact with PVC film. The migration of NP in sample is indicated as 'outside of rice' according to the outward of samples and total migration levels per 10 g by the calculation according to the measurement of the inward and outward of sample. Furthermore, based on our residue test, we investigated only these four films from same residue range levels.

Results and discussion

LC/ED analytical performance

ED was employed in order to utilize the well-known electro-activity of the phenolic group present in the NP molecule. Phenolic oxidation potentials generally shift to more negative values with an increase in pH, therefore we chose to include phosphoric acid in the mobile phase. Thus, acetonitrile–phosphoric acid in water was used for the mobile phase and the sensitivity of detection was optimized by altering the concentration of phosphoric acid. Hydrodynamic voltammograms of authentic NP standard at various concentrations of phosphoric acid are shown in figure 1. The 0.5% phosphoric acid showed good sensitivity, with a detection limit of 1.0 ng/ml with S/N = 3. The calibration curve for the NP standard constructed by plotting the concentration versus the peak area showed a good linearity in the range of 10–1000 ng/ml ($r^2 = 0.998$). When the NP standard and the residue sample was consecutively measured, the retention times were 9.6 min with good separation (figure 2). Confirmation of results was carried out by comparing the ratio (R) between a standard and the actual sample. The R value of the authentic NP standard was 40.1 and that of the residue sample (from PVC film No.1) was 39.3, confirming that the peak in the residue sample is due to NP.

Residues of NP in PVC films

The levels of NP in the PVC films intended for food-packaging are shown in table 1 and were in the range of not detected (< 500 µg/g) to 3300 µg/g. The highest amount was in one of the films intended for home-use

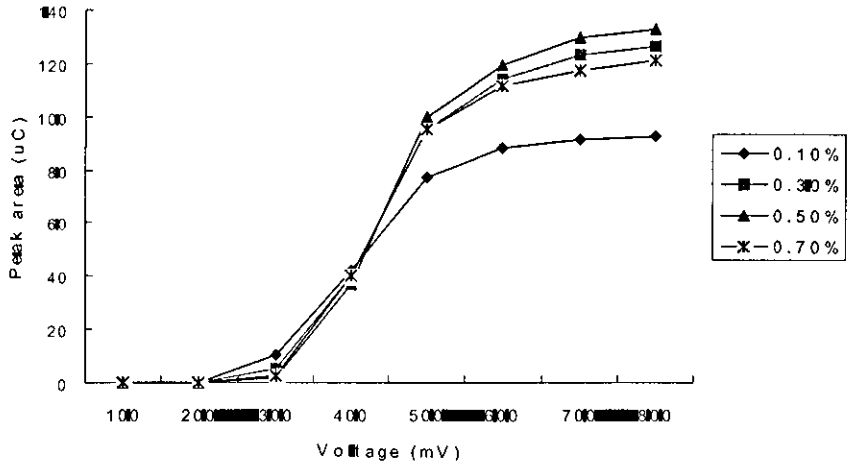

Figure 1. Hydrodynamic voltammograms of NP (1000 ng/ml) for mobile phase. Applied voltage; Ch_1 (50 mV) Ch_2 (detector voltage). Mobile phase: acetonitrile and 0.1–0.7% phosphoric acid in water.

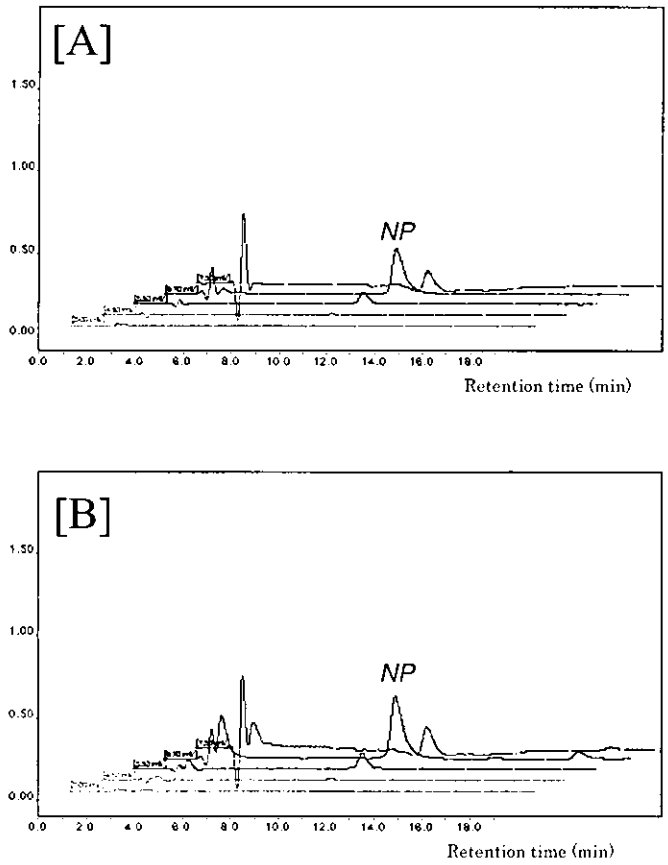

Figure 2. LC/ED chromatograms of standard and residue sample from PVC film. [A]: Standard of NP (500 ng/ml) R = 40.1. [B]: Residue sample (PVC film of sample No.1) R = 39.3.

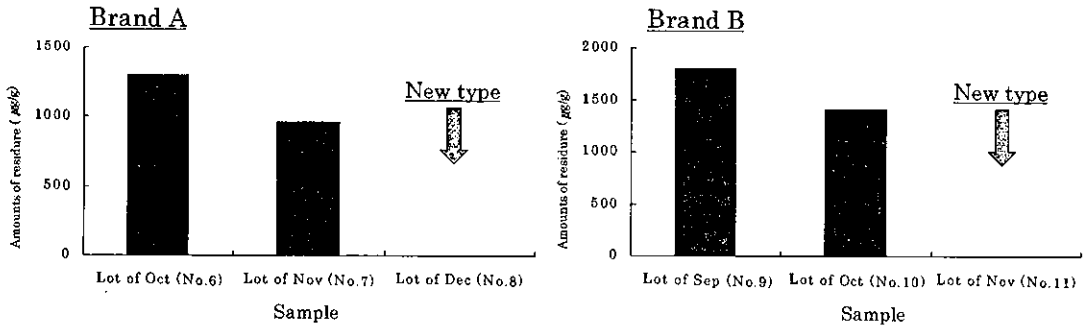

Figure 3. Comparison of residue in PVC films from different productive lots. The comparison of residue NP from old versus new batches of PVC films.

Table 1. Residue of NP in PVC films for food-wrapping.

Residue range (μg/g)	Detection of sample No. (μg/g)
> 2000	No. 14(3300)
1900–1500	*No. 9(1800)*
1400–1000	*No. 1(1400), No. 4 (1200), No. 6(1200)*
	No. 7 (1000), No. 10(1400), No. 13 (1200)
900–500	*No. 2(650), No. 3(830), No. 12(500)*
ND (< 500)	*No. 5, No. 8, No. 11*, No. 15–22

Home-use type: normal font.
Retail-use type: Italic font.

but many of the films intended for retail-use also contained NP. On investigation of NP levels in the different of PVC films, it was found that NP was not detected in the new type of PVC films. It was thought that PVC film manufacturers had changed to the new type of films for safety reasons.

Non-ionic surfactants based on nonylphenol polyethoxylates are widely used by the textile and pulp and paper industries. Polyethylene glycol ethers of nonylphenol are frequently used as emulsifiers. However, it is not likely that the presence of NP is due to its presence as a contaminant as in the worst case the PVC contains only 0.33% of NP. The migration of NP (and NP as a degradation product) from tris(nonylphenoyl) phosphite into food simulants from PVC materials is not an unexpected finding.

Migration test of NP from PVC films

Table 2 shows that up to 1.6 μg/cm^2 of NP migrated from the PVC films into the *n*-heptane. This level was higher than that migrating into distilled water and 4% acetic acid. The amount of NP migrating into distilled water and 4% acetic acid was in the range not detected—9.7 ng/cm^2 (not detected = < 1.0 ng/cm^2).

The relationship between the migration of NP from the PVC films into *n*-heptane (60 min, 25°C) and the residue of NP in the PVC films is shown in figure 4. A correlation of $R^2 = 0.8798$ was observed, therefore the residue of NP in the PVC films (μg/g) was related to the NP migration levels from the PVC films. All film samples were of similar thickness, about 0.7 mg/cm^2. Migration into distilled water and 4% acetic acid was at levels up to 0.23% (No. 0, 4% acetic acid), and into *n*-heptane at levels up to 62.5% (No. 2).

Exposure of PVC films to food

The method used for the extraction of NP from the rice was chosen for its convenience. The rice samples for recovery tests and for exposure to NP were cooked. The chromatographic resolution achieved

Table 2. Migration test of NP in PVC films for food-wrapping.

Sample (No.)	Type	*n*-Heptane[a] ($\mu g/cm^2$)	Water[b] (ng/cm^2)	AcOH[c] (ng/cm^2)
1	Retail	0.89	2.3	3.5
2	Retail	0.58	ND	ND
3	Retail	0.64	ND	ND
4	Retail	0.75	2.2	1.5
5	Retail	ND	ND	ND
6	Retail	0.92	1.5	3.2
7	Retail	0.69	ND	ND
8	Retail	ND	ND	ND
9	Retail	1.13	3.5	1.5
10	Retail	1.01	3.2	4.5
11	Retail	ND	ND	ND
12	Retail	0.33	ND	ND
13	Home	0.53	ND	ND
14	Home	1.6	9.7	7.2
15	Home	ND	ND	ND
16	Home	ND	ND	ND
17	Home	ND	ND	ND
18	Home	ND	ND	ND
19	Home	ND	ND	ND
20	Home	ND	ND	ND
21	Home	ND	ND	ND
22	Home	ND	ND	ND

[a] *n*-Heptane (25°C, 60 min); unit: $\mu g/cm^2$; ND < 1.0 $\mu g/cm^2$.
[b] Water (60°C, 30 min; unit: ng/cm^2; ND < 1.0 ng/cm^2.
[c] 4% AcOH (60°C, 30 min; unit: ng/cm^2; ND < 1.0 ng/cm^2.

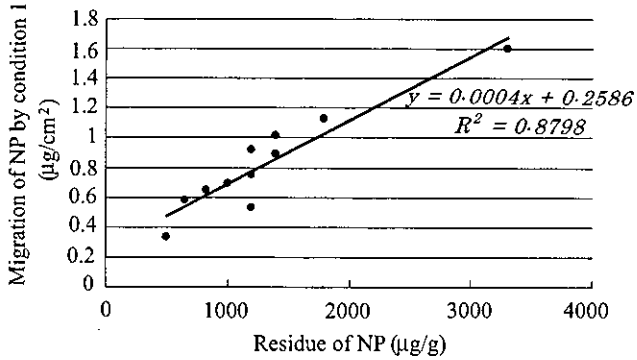

Figure 4. Correlation between results from the residue tests and migration test (n-heptane, 25 °C, 60 min).

was quite adequate, as shown in figure 5, and replicate recoveries were 86.3%, 86.2%, 83.3%, 81.4% and 81.2%. The average recovery was 83.7% with a standard deviation of 2.5%. The result of recovery tests suggested that the method could be successfully applied for the monitoring of NP in the rice samples.

The migration of NP from PVC films to rice samples is shown in table 3, for PVC films No. 14, 9, 1 and 16. These results indicate a maximum migration of NP into cooked rice of 171.8 ng/g. If a person with a 50 kg body weight takes 200 g of rice per day, the total amount of NP ingested per day is 0.7 $\mu g/kg$ bw/day (171.8 ng/g × 200 g/50 kg). This estimated intake indicates a safety margin of about 70 000 taking into account the highest intake of NP and a NOAEL of 50 mg/kg bw/day (Chapin *et al.* 1999 and Cunny *et al.* 1997). Other reports and this

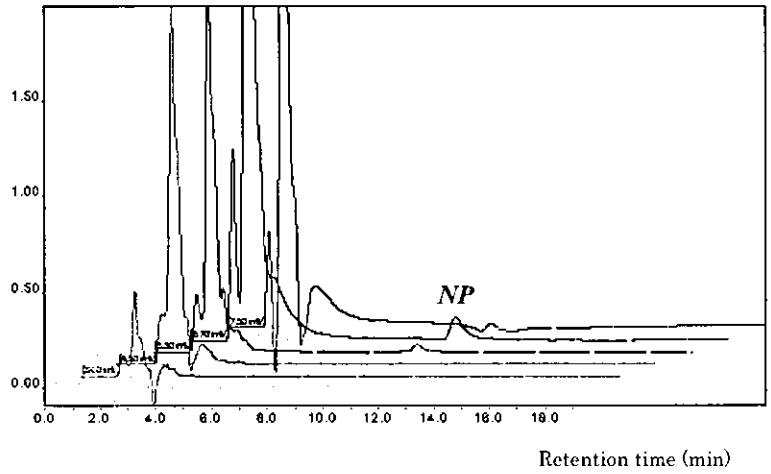

Figure 5. LC/ED chromatograms of rice sample wrapped in PVC film. The rice sample wrapped in PVC film is sample No. 2 taken from the outside.

Table 3. Migration of NP into PVC films to food (rice sample).

	Content in rice (ng/g)			
	Outside of rice		Total	
Sample No.	Case 1	Case 2	Case 1	Case 2
Control	ND	ND	ND	ND
14	410.0	76.5	171.8	35.0
9	80.6	19.0	34.3	7.6
1	57.3	13.1	24.4	5.2
16	ND	ND	ND	ND

Not detected (ND) < 1.0 ng/g.

result lead to the conclusion that there is little need to be concerned about NP exposure from the diet at present (Toppari *et al.* 1996).

Conclusions

An HPLC method has successfully been applied to the analysis of NP in PVC films and to study migration into food simulants and rice. Some PVC films contained NP at concentrations of between 500 and 3300 μg/g. The migration of NP from the PVC films was influenced by the test conditions (*n*-heptane at 25°C for 60 min, distilled water at 60°C for 30 min and 4% acetic acid at 60°C for 30 min). The amounts of NP (0.33–1.6 μg/cm^2) migrating from PVC films into *n*-heptane were higher than those migrating into distilled water and 4% acetic acid (not detected—9.7 ng/cm^2).

Acknowledgement

This work was supported by Health Sciences Research grants from the Ministry of Health and Welfare of Japan.

References

ACHILLI, G., CELLERIO, G. P., MELZI D'ERIL, G. V., and BIRD, S., 1995, Simultaneous determination of 27 phenols and herbicides in water by high-performance liquid chromatography with multi-electrode electrochemical detection. *Journal of Chromatography A*, **697**, 357–363.

ACHILLI, G., CELLERIO, G. P., MELZI D'ERIL, G. V., and TAGLIARO, F., 1996, Determination of illicit drugs and related substances by high-performance liquid chromatography with an electrochemical coulometric-array detector. *Journal of Chromatography A*, **729**, 273–277.

CASTLE, L., MERCER, A. J., STARTIN, J. R., and GILBERT, J., 1987, Migration from plasticized films into foods. 2. Migration of di-(2-ethylhexyl) adipate from PVC films used for retail food packaging. *Food Additives and Contaminants*, **4**, 399–406.

CHAPIN, R. E., DELANEY, J., WANG, Y., LANNING, L., DAVIS, B., COLLONS, B., MINTZ, N., and WOLFE, G., 1999, The effects

of 4-nonylphenol in rats: a multigeneration reproduction study. *Toxicological Sciences*, **52**, 80–91.

CUNNY, H. C., MAYERS, B. A., ROSICA, K. A., TRUTTER, J. A., and VAN MILER, J. P., 1997, Subchronic toxixity (90-day) study with *para*-nonylphenol in rats. *Regulatory Toxicology and Pharmacolgy*, **26**, 172–178.

DING, W. H., and TZING, S. H., 1998, Analysis of nonylphenol polyethoxylates and their degradation products in river water and sewage effluent by gas chromatography–ion trap (tandem) mass spectrometry with electron impact and chemical ionization. *Journal of Chromatography A*, **16**, 79–90.

KAWAMURA, Y., TAGAI, C., MAEHARA, T., and YAMADA, T., 1999a, Additives in polyvinyl chloride and polyvinylidene chloride products. *Journal of Food Hygienic Society of Japan*, **4**, 274–284.

KAWAMURA, Y., TAGAI, C., MAEHARA T., and YAMADA, T., 1999b, Simultaneous determination method of additives in polyvinyl chloride. *Journal of Food Hygienic Society of Japan*, **3**, 189–197.

MARCOMINI, A., CAPRI, S., and GIGER, W., 1987, Determination of linear alkylbenzenesulphonates, alkylphenol polyethoxylates and nonylphenol in waste water by high-performance liquid chromatography after enrichment on octadecylsilica. *Journal of Chromatography*, **21**, 243–252.

PETERSEN, J. H., and BREINDAHL, T., 1998, Specific migration of di-(2-ethylhexyl) adipate (DEHA) from plasticized PVC film: results from an enforcement campaign. *Food Additives and Contaminants*, **5**, 600–608.

RIZZO, V., MELZI D'ERIL, G., ACHILLI, G., and CELLERINO, G. P., 1991, Determinaton of neurochemcals in biological fluids by using an automated high-performance liquid chromatographic system with a coulometric detector. *Journal of Chromatography*, **536**, 229–236.

SASAKI, K., TAKATSUKI, S., NEMOTO, S., IMANAKA, M., ETO, S., MURAKAMI, E., and TOYODA, M., 1999, Determination of alkylphenols and 2,4-dichlorophenol in foods. *Journal of Food Hygienic Society of Japan*, **6**, 460–472.

SOTO, A. M., JUSTICIA, H., WRAY, J. W., and SONNENSHEIN, C., 1991, *p*-Nonylphenol: an estrogenic xenobiotic released from 'modified' polystyrene. *Environmental Health Perspectives*, **92**, 167–173.

STARTIN, J. R., SHARMAN, M., ROSE, M. D., PARKER, I., MERCER, A. J., CASTLE, L., and GILBERT, J., 1987, Migration from plasticized films into foods. 1. Migration of di-(2-ethylhexyl) adipate from PVC films used for retail food packaging. *Food Additives and Contaminants*, **4**, 385–398.

TOPPARI, J., LARSEN, J. C., CHRISTIANSEN, P., GIWERCMAN, A., GRNDJEAN, P., GUILLETTE, L. J., JR, JEGOU, T. K., JOANNET, P., KEIDING, N., LRFFERS, H., MCLACHLAN, J. A., MEYER, O., MULLER, J., RAJPERT-DE MEYTS, E., SCHEIKE, T., SHARPE, R., SUMPTER, J., and SKAKKEBAEK, N. E., 1996, Male reproductive health and environmental estrogens. *Environmental Health Perspectives*, **104**, 741–803.

TSUDA, T., TAKINO, A., KOJIMA, M., HAADA, H., and MURAKI, K., 1999, Gas chromatographic-mass spectrometric determination of 4-nonylphenols and 4-*tert*-ocylphenol in biological samples. *Journal of Chromatography B*, **723**, 273–279.

WHITE, R., JOBLING, S., HOARE, S. A., SUMPTER, J. P., and PARKER, M. G., 1994, Environmentally persistent alkylphenolic compounds are estrigenic. *Endocrinology*, **135**, 175–182.

Original

[*Journal of Environmental Chemistry* Vol.11, No.3, pp.517-523, 2001]

Analysis of Chlorobenzenes in Blood by Head Space SPME-GC/MS

Tadashi TSUKIOKA[1], Jun-ichi TERASAWA[1], Tetsuya YOSHIDA[1], Moritoshi SATO[1], Hiromichi FUJISHIMA[1], Hiroyuki NAKAZAWA[2] and Tsunehisa MAKINO[3]

[1]Nagano Research Institute for Health and Pollution
(1978 Amori, Komemura, Nagano 380-0944)
[2]Hoshi University
(2-4-41 Ebara, Shinagawa-ku, Tokyo 142-8501)
[3]Tokai University
(Bouseidai, Isehara, Kanagawa 259-1193)

[Received April 23, 2001]

Summary

We have developed a method for the determination of chlorobenzenes in blood by head space SPME-GC/MS. Five mℓ of blood sample is put into a head space bottle, to which an enzyme is added for proteolysis. The head space of the bottle is sampled by a solid phase micro extraction (SPME). The SPME fiber is analyzed for chlorobenzenes by GC/MS. This method is excellent in sensitivity and selectivity, easy to operate, and is applicable to actual samples. This is also an environmentally friendly method, for it requires only small amounts of reagents and solvents.

Blood samples were collected from 60 subjects, all of whom are members of Nagano Research Institute for Health and Pollution and their families, and analyzed. In all the blood samples, *p*-dichlorobenzene (0.4～210 ppb; 14.9 ppb on the average) and HCB (0.07～0.40 ppb; 0.17 ppb on the average) were detected. *p*-Dichlorobenzene is considered to have been derived from moth-proofing agents for clothes and odor-removing agents for toilets, whereas HCB is considered to have been derived from food.

Key words: endocrine disruptor, HCB, *p*-dichlorobenzene, SPME-GC/MS, blood

INTRODUCTION

Chlorobenzenes, a group of 12 members, ranging from monochlorobenzene to hexachlorobenzene, have been widely used as intermediates for organic syntheses, pesticides and fungicides. Of these chlorobenzenes, hexachlorobenzene (HCB) is considered to be as an endocrine disruptor[1]. According to studies conducted by Ministry of the Environment of Japan (MOE), *p*-dichlorobenzene (*p*-DCB), 1,2,3- and 1,2,4-trichlorobenzene, pentachlorobenzene and HCB were detected in bottom sediments and organisms[2]. HCB was used as a fungicide, but it has never been registered as an agricultural chemical in Japan. Accordingly, the HCB detected may have been derived from impurities in agricultural chemicals such as pentachloronitrobenzene and pentachlorophenol, and by-products from processes for producing organic solvents. In Turkey in the 1950s, of those who ate wheat seeds previously treated with HCB, 3000～5000 people suffered from porphyria, and about 400 died[3]. A relatively large number of reports have been made on HCB contents in breast milk[4-10]. A study in the early 1990s revealed that the average HCB content in

human milk (fat basis) was 826 ppb for subjects in West Germany, 140 ppb in Britain, 110 ppb in Norway, 84 ppb in Turkey, 54 ppb in Canada, and 31 ppb in the U.S.[4]. In contrast, there was little study on HCB in blood[5]. Since chlorobenzenes may be taken from food and air, it is necessary to find out accurately to what extent humans are exposed to chlorobenzenes.

Several analytical methods have been proposed for chlorobenzenes in biological samples[13-19]. In those methods, samples are subjected to alkali digestion in a circulating steam distillation equipment, then extracted into *n*-hexane, and determined by GC-ECD[13]. Roehrig Lars et al. proposed a method in which chlorophenols, HCH, DDT, and HCB in blood samples are subjected to SPME followed by a determination by GC-ECD[14]. A method using GC/MS was proposed in a tentative manual for research of exogenous endocrine disrupting chemicals by MOE[15]. As well, Barr et al. proposed a method in which chlorobenzenes from human samples were subjected to isotope dilution GC/MS[16]. Among biological samples, blood samples have been difficult to analyze by conventional methods, due to insufficient sensitivities and selectivities of the methods. A large volume of blood is needed to satisfy the detection limit of 100 ppt. To overcome these problems, we have developed a method for determining chlorobenzenes in biological samples such as blood and breast milk by use of head space SPME-GC/MS. We then applied the method to analyze chlorobenzenes in blood of adults (n=60). As a result, *p*-DCB was detected in all blood samples with average concentration of 14.9 ppb. To identify the cause, we measured the concentration of *p*-DCB in indoor air and analyzed the relationship between the concentration of *p*-DCB in indoor air and blood.

EXPERIMENT

Reagents

All the 12 chlorobenzenes and Proteinase K were purchased from Wako Pure Chemical Industries, Ltd. $^{13}C_6$ labeled HCB and d_4 labeled *p*-dichlorobenzene (DCB) were purchased from Cambridge Isotope Laboratories, Inc..

The Passive Gas Tubes containing activated charcoal (200mg in 20~40 mesh) were purchased from Sibata Co., Ltd..

Collection of blood samples

Human blood samples were collected from members of staff at Nagano Research Institute for Health and Pollution and their families (n=60) into vacutainer containing heparin (10 mℓ), shaken vigorously and stored in a refrigerator at 5 ℃ until analysis; the blood sampling was preceded by the due procedure for informed consent. Blood samples from cattle were collected at a slaughter house in Nagano Prefecture. Heparin was added, and stored in a freezer at −20 ℃.

Equipments and apparatuses

Head space bottles (22 mℓ), Techmar (USA), SPME fibers 65 μm of polydimethylsiloxane-divinylbenzene film, Supelco (USA), and blood collecting tube (Beneject II, 10 mℓ, Terumo, Tokyo) were used.

GC/MS conditions

GC/MS conditions were listed as follows:

GC: HP-5890 (Agilent, USA)

MS: GC-mate (JEOL, Ltd.)

Column: HP-5, 0.32 mm×30 m×0.52 μm (Agilent, USA)

Oven temperature: 50 ℃ (2 min)−8 ℃/min−250 ℃ (5 min)

Inlet temperature: 250 ℃

Ion source temperature: 250 ℃

Ionization current: 300 μA

Ionization voltage: 70 V

Ionization method: EI+

Measuring method: SIM

Carrier gas: He at 1 mℓ/min

Monitor ions (m/z): 112 and 114 (chlorobenzene), 146 and 148 (dichlorobenzene), 152 (*p*-dichlorobenzene-d_4), 180 and 182 (trichlorobenzene), 214 and 216 (tetrachlorobenzene), 248 and 250 (pentachlorobenzene), 284 and 286 (HCB), and 292 ($^{13}C_6$-HCB).

Analyses

Measurement of concentrations in blood

Five ml of human blood was taken into a vial for head space with a capacity of 22 mℓ, to which Proteinase K (200 units), HCB-$^{13}C_6$ (5 ng), and *p*-DCB-d_4 (20 ng) were added. The vial was tightly closed with a stopper, and heated for 3 h at 60 ℃. Then,

an SPME fiber was kept immersed into the head space bottle for 30 min at 80 ℃ to extract chlorobenzenes, and subjected to a measurement by GC/MS-SIM.

Calibration curve: 5 mℓ of blood from cattle was taken into a vial bottle for head space, to which chlorobenzenes were added at a concentration range of 0.25~25 ng. The mixture was treated in the same manner as described above, and the concentrations were evaluated from the area relative to surrogate compounds.

Measurement of the p-dichlorobenzene concentration in indoor air

p-DCB was absorbed by activated charcoal in a passive tube attached to the breast of an individual for two days, to measure human exposures via air. The passive tube was also placed in a bedroom and in a living room for two days. After two days, the activated charcoal in the passive tube was taken out into a vial, to which 2 mℓ of carbon disulfide was added. The mixture was shaken and allowed to stand for 2 h. *p*-DCB-d_4 was added to the mixture as an internal standard. The resultant mixture was analyzed by GC/MS-SIM and the concentration of *p*-DCB was determined based on its area relative to the internal standard.

RESULTS AND DISCUSSION

Method development

Storage of samples

Previous to this study, it has been confirmed that the measurement would not be disturbed by anticoagulants, EDTA and heparin. Thus, we decided to use commercial blood collecting tubes containing heparin. Collected blood was shaken well and stored in a refrigerator until analysis at 5 ℃.

Proteolytic enzyme

If the blood temperature is raised to 80 ℃ during the analytical process, some proteins may become solid which leads to a significant decrease in the extraction efficiency by SPME fiber. To prevent it, Proteinase K was added to 5 mℓ of cattle blood gradually and decomposed proteins for 30 min at 60 ℃. The result showed that addition of 100 units of Proteinase K to 5 mℓ of cattle blood satisfactorily prevented the solidification of proteins. In the following analysis, 200 units of Proteinase K was added to all samples.

Selection of SPME fiber

One hundred μm film thickness of polydimethylsiloxane (PDMS), 65 μm film thickness of polydimethylsiloxane-divinylbenzene (PDMS-DVB), 75 μm film thickness of Carboxen-polydimethylsiloxane (Carboxen-PDMS), and 65 μm film thickness of Carbowax-divinylbenzene (CW-DVB) were compared to attain the highest extraction efficiency of the substances. PDMS-DVB and CW-DVB showed good performances, while Carboxen-PDMS, though adsorbing mono-and DCBs, showed unsatisfactory desorption and severely tailing peaks. Thus, PDMS-DVB was selected for this in this study.

SPME conditions

To select optimum temperature and extraction time on the SPME fiber, 5 ng of standards were added to 5 mℓ of cattle blood treated with Proteinase K. The condition changed in the range of 50~100 ℃ and 5~50 min. The results showed that the recovery of HCB, which has a higher boiling point, was higher at higher temperatures, whereas the recovery of mono- and DCBs decreased. The SPME condition of 30 min. at 80 ℃ was chosen after due consideration.

GC/MS conditions

By using an HP-5 column, which is a weak polar column, all the target compounds could be separated, except 1,2,3,5- and 1,2,4,5-tetrachlorobenzene. Molecular ions and one fragment ion were monitored for measurement. *p*-DCB-d_4 and HCB-$^{13}C_6$ were used as surrogates. The monitor ion of m/z=292 was used though it had a base peak at m/z=290 because the ion channel can be affected when the HCB concentration is high. Figure 1 shows SIM chromatograms of chlorobenzenes.

Table 1 shows the detection limits and calibration ranges for chlorobenzenes. The detection limits were evaluated from S/N=3, with 5 mℓ of cattle blood used. The detection limit of monochlorobenzene was 0.1 ppb, a relatively higher value, but the detection limits of the other compounds were satisfactory. The reproducibility of the present analytical method was checked by applying the method to 5 mℓ of cattle blood sample having chlorobenzenes added to 0.5 ppb. The relative standard deviations obtained were 2.2~8.0% as shown in Table 2. Figure 2 shows SIM chromatograms of a blood sample. In the blood sample, *p*-DCB (6.3 ppb) and HCB (0.16 ppb) were detected.

In this study, it was proved that the head space-

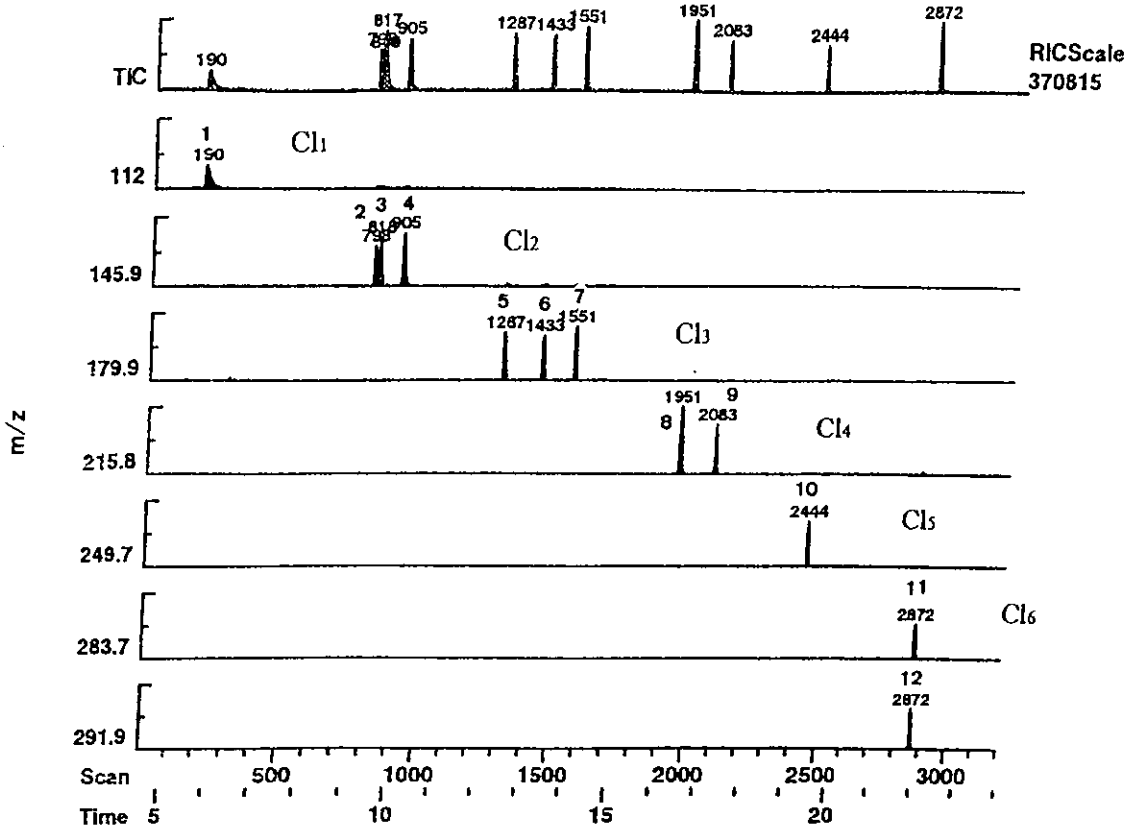

Fig. 1 SIM chromatograms of chlorobenzenes

Peaks: 1, monochlorobenzene; 2, *m*-DCB; 3, *p*-DCB; 4, *o*-DCB; 5, 1,3,5-trichlorobenzene (TCB); 6, 1,2,4-TCB; 7, 1,2,3-TCB, 8, 1,2,3,5-Tetrachlorobenzene(TeCB)+1,2,4,5-TeCB; 9, 1,2,3,4-TeCB; 10, Pentachlorobenzene; 11, HCB; 12, $^{13}C_6$-HCB

Table 1 Detection limits and calibration ranges for chlorobenzenes

Compound	D.L. (ppb)	Calibration range (ppb)
Chlorobenzene	0.10	0.1-20
o-Dichlorobenzene	0.01	0.01-20
m-Dichlorobenzene	0.01	0.01-20
p-Dichlorobenzene	0.01	0.01-20
1,2,3-Trichlorobenzene	0.01	0.01-20
1,2,4-Trichlorobenzene	0.01	0.01-20
1,3,5-Trichlorobenzene	0.01	0.01-20
1,2,3,4-Tetrachlorobenzene	0.01	0.01-10
1,2,3,5-Tetrachlorobenzene	0.01	0.01-10
1,2,4,5-Tetrachlorobenzene	0.01	0.01-10
Pentachlorobenzene	0.02	0.02-10
Hexachlorobenzene	0.02	0.02-10

Table 2 Results of the reproducibility test on chlorobenzenes

Compound	R.S.D.(%)
Chlorobenzene	3.5
o-Dichlorobenzene	3.9
m-Dichlorobenzene	2.7
p-Dichlorobenzene	3.0
1,2,3-Trichlorobenzene	4.1
1,2,4-Trichlorobenzene	4.9
1,3,5-Trichlorobenzene	4.6
1,2,3,4-Tetrachlorobenzene	8.0
1,2,3,5-Tetrachlorobenzene	6.2
1,2,4,5-Tetrachlorobenzene	5.7
Pentachlorobenzene	5.0
Hexachlorobenzene	2.2
	(n=5)

SPME-GC/MS method has sensitivity and easiness of operation for analysis of biological samples which are available in small amount and may be hazardous in some disease cases.

Concentrations in human blood

The chlorobenzenes detected from the blood samples were *p*-DCB (0.4~210 ppb; 14.9 ppb on the average) and HCB (0.07~0.40 ppb; 0.17 ppb on the average). Figure 3 shows the relationship between the concentrations of *p*-DCB in indoor air and in blood. *p*-

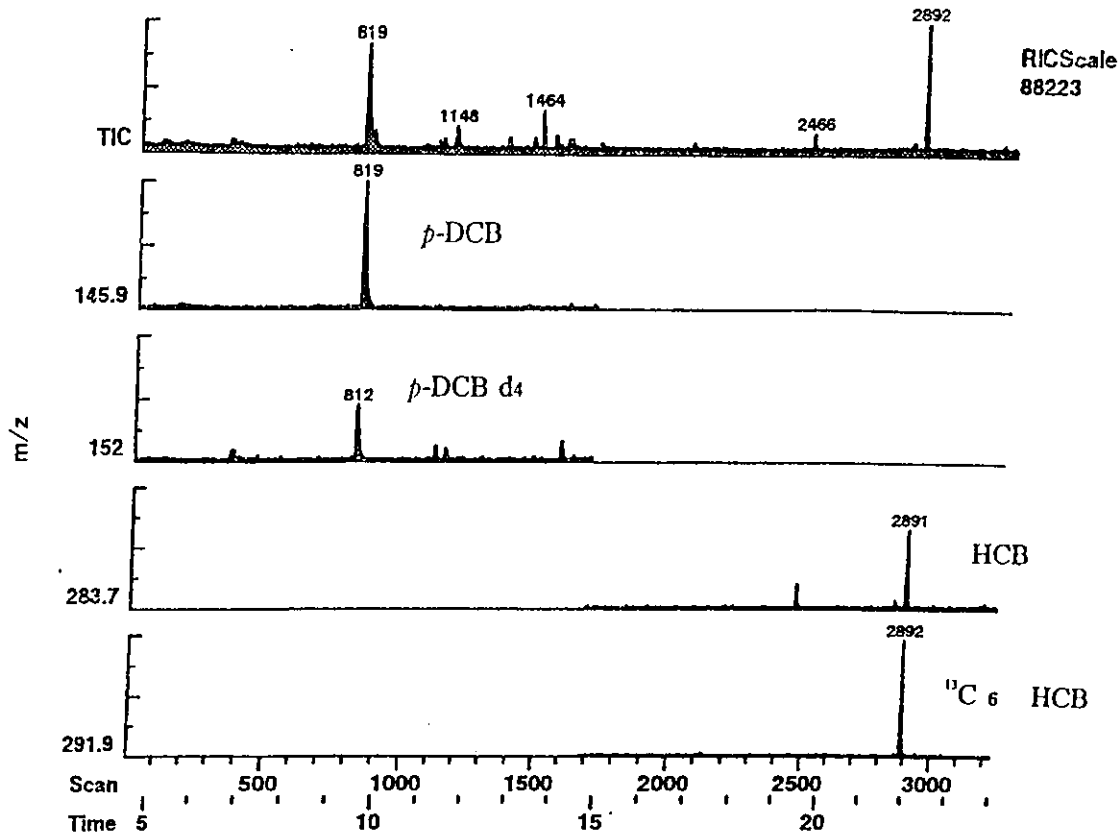

Fig. 2 SIM chromatograms of blood sample

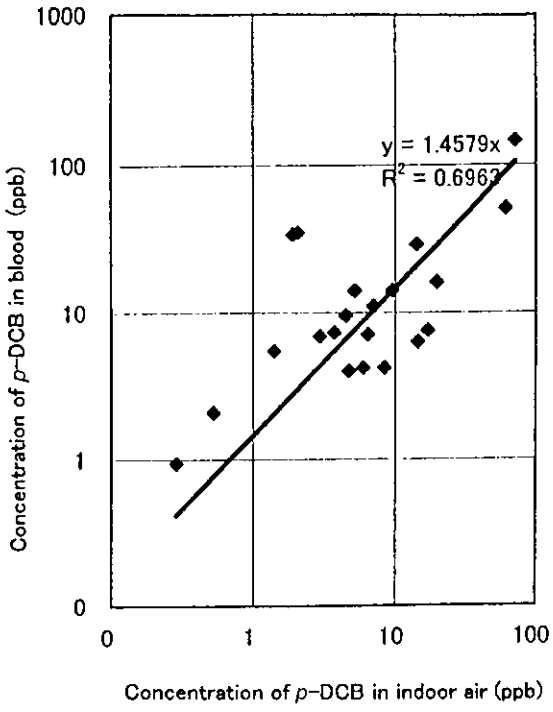

Fig. 3 Relationship between the concentration of *p*-dichlorobenzene in indoor air and in blood

DCB was detected in all the blood samples at 14.9 ppb on the average. Since *p*-DCB is widely used as a moth-proofing agent for clothes and odor removing agents for toilets, it is possibly absorbed from surrounding air by respiration. The concentration of *p*-DCB in indoor air and that in blood are correlated. Among the members of the same family, the blood samples from members, who live longer at home, showed higher concentrations of *p*-DCB.

HCB was also detected in all the blood samples at 0.17 ppb on the average. A histogram (Fig. 4) showing a relatively normal distribution was obtained. The concentrations of HCB were comparable to those reported in Canada (0.11~0.34 ppb)[5]. According to the survey by the Ministry of Environment of Japan, it is supposed that HCB is taken mostly via foods, mainly fish.

ACKNOWLEGEMENTS

This study was supported by Health Sciences Research Grants, the Ministry of Health and Welfare of Japan (The study of the effect on the fetus and adult from the exposure of endocrine disrupting

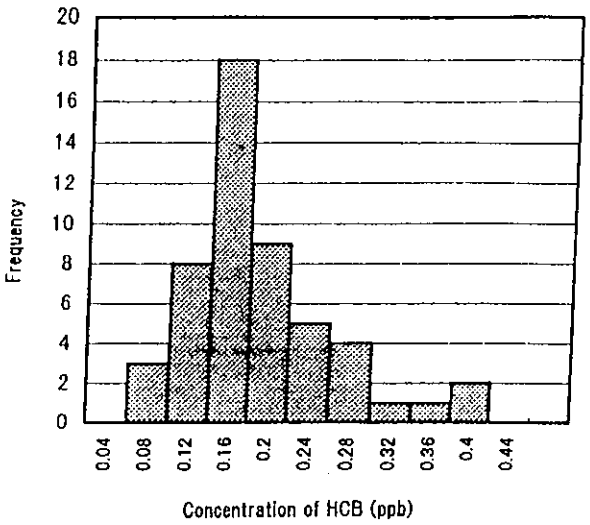

Fig. 4 Histogram of HCB in human blood (n=60)

chemicals), from 1998 to 1999. We would like to thank the members of the Infectious Disease Division of Nagano Research Institute for Health and Pollution who helped collect the blood, as well as those members and their families who were generous enough to offer their bloods for this study.

REFERENCES

1) EPA Special Report on Environmental Endocrine Disruption: An effect assessment and analysis, p111, Feb. (1997)
2) The Environmental Agency of Japan: Chemicals in the environment, 450-503 (1999)
3) Wakatsuki, T., Matsusima, S. and Ando, M.: Toxicity of pesticides and the influence of it on the health, p134, Kougai Taisaku Senta (1989)
4) H. Basri U.M., M. Adnan O., Hasanoglu, E. and Dogan, M.: Organochlorine pesticide residues in human milk in Kayseri. *Human & Experim. Toxicol.*, **13**, 99-302 (1994)
5) Jos, M.: Organochlorine residues in human blood and biopsy fat and their relationship. *Bull. Environ. Contam. Toxicol.*, **48**, 815-820 (1992)
6) Schade, G. and Heinzow, B.: Organochlorine pesticides and polychlorinated biphenyls in human milk of mothers living in northern Germany: Current extent of contamination, time trend from 1986 to 1997 and factors that influence the levels of contamination. *Sci. Total Environ.*, **215 (1,2)**, 31-39 (1998)
7) Silva, A.S., Barretto, H.H.C., Lemes, R.R., and Kussumi, T.A.: Determination of human exposure to hexachlorobenzene at organochlorine industry chemical residue sites located in Samoria, Sao Vicete, Sao Paulo, Brazil. *Pesticidas,* **7**, 123-135 (1997)
8) Waliszewski, S.M., Pardio, V.T., Aguirre, A.A., Coronel, H., Infanzon, R.M. and Rivera, J.: Persistent organochlorine pesticides in bovine meat and milk from Veracruz. *Organohalogen Compd.*, **32**, 335-339 (1997)
9) Atuma, S.S., Hansson, L., Johnsson, H., Slorach, S., de Wit, C.A. and Lindstrom, G.: Organochlorine pesticides, polychlorinated biphenyls and dioxins in human milk from Swedish mothers. *Food Addit. Contam.*, **15 (2)**, 142-150 (1998)
10) Skaare, J.U., Tuveng, J.M. and Sande, H.A.: Organochlorine pesticides and polychlorinated biphenyls in maternal adipose tissue, blood, milk, and cord blood from mothers and their infants living in Norway. *Arch. Environ. Contam. Toxicol.*, **17 (1)**, 55-63 (1988)
11) Jemaa, Z., Sabbah, S., Driss, M.R. and Bouguerra, M.L.: Hexachlorobenzene in Tunisian mothers' milk, cord blood and foods. *IARC Sci. Publ.*, **77**, 139-142 (1986)
12) Ando, M., Hirani, S. and Itoh, H.: Transfer of hexachlorobenzene (HCB) from mother to newborn baby through placenta and milk. *Arch. Toxicol.*, **56 (3)**, 195-200 (1985)
13) Mckenzie, C., Rogan, E., Reid, R.J. and Wells, D. E.: Concentrations and patterns of organic contaminants in Atlantic white-sided dolphins (Lagenorhynchus acutus) from Irish and Scottish coastal waters. *Environ. Pollut.* **98 (1)**, 15-27 (1998)
14) Tsukioka, T. and Shimizu, S.: A simple analytical method for chlorobenzenes in biological samples. *Bull. Nagano Research Institute for Health and Pollution*, **3**, 16-19 (1981)
15) Roehrig, L., Puttmann, M. and Meisch, H.-U.: Determination of persistent organochlorine compounds in blood by solid phase micro extraction and GC-ECD. *Fresenius' J. Anal. Chem.*, **361 (2)**, 192-196 (1998)
16) The Environmental Agency of Japan: Tentative manual for research of exogenous endocrine disrupting chemicals (water quality, bottom sediment, living body), II, 1-16 (1998)
17) Barr, J.R., Barr, D.B., Patterson, D. Jr., Needhan,

L.L. and Bond, A.E.: Quantification of non-persistent pesticides in human samples by isotope dilution mass spectrometry. *Toxicol. Environ. Chem.*, **66 (1-4)**, 3-10 (1998)

18) Okor, D.I. and Atuma, S.S.: Determination of organochlorine residues in maternal and cord blood plasma. *Int. J. Environ. Anal. Chem.*, **33 (2)**, 141-147 (1988)

19) Ando, M., Saito, H. and Wakisaka, I.: Gas chromatographic and mass spectrometric analysis of polychlorinated biphenyls in human placenta and cord blood. *Environ. Res.*, **41 (1)**, 14-22 (1986)

A basolateral sorting motif in the MICA cytoplasmic tail

Hiroshi Suemizu*†, Mirjana Radosavljevic‡, Minoru Kimura*, Sotaro Sadahiro§, Shinichi Yoshimura*, Seiamak Bahram‡¶, and Hidetoshi Inoko*¶

*Department of Genetic Information and §Department of Surgery, Tokai University School of Medicine, Bohseidai, Isehara 259-1193, Japan; †Central Institute for Experimental Animals, Nogawa 1430, Miyamae, Kawasaki 216-0001, Japan; and ‡Institut National de la Santé et de la Recherche Médicale–Contrat de Recherche Stratégique, Centre de Recherche d'Immunologie et d'Hématologie, 4 Rue Kirschleger, 67085 Strasbourg, France

Communicated by Pamela J. Bjorkman, California Institute of Technology, Pasadena, CA, December 26, 2001 (received for review November 6, 2001)

The MHC class I chain-related MICA molecule is a stress-induced, highly polymorphic, epithelia-specific, membrane-bound glycoprotein interacting with the activating NK cell receptor NKG2D and/or gut-enriched Vδ1-bearing γδ T cells. We have previously reported the presence of a MICA transmembrane-encoded short-tandem repeat harboring a peculiar allele, A5.1, characterized by a frame shift mutation leading to a premature intradomain stop codon, thus denying the molecule of its 42-aa cytoplasmic tail. Given that this is the most common population-wide MICA allele found, we set out to analyze the functional consequences of cytoplasmic tail deletion. Here, we show native expression of MICA at the basolateral surface of human intestinal epithelium, the site of putative interaction with intraepithelial T and NK lymphocytes. We then demonstrate, in polarized epithelial cells, that although the full-length MICA protein is sorted to the basolateral membrane, the cytoplasmic tail-deleted construct as well as the naturally occurring A5.1 allele are aberrantly transported to the apical surface. Site-directed mutagenesis identified the cytoplasmic tail-encoded leucine-valine dihydrophobic tandem as the basolateral sorting signal. Hence, the physiological location of MICA within epithelial cells is governed by its cytoplasmic tail, implying impairment in A5.1 homozygous individuals, perhaps relevant to the immunological surveillance exerted by NK and T lymphocytes on epithelial malignancies.

Conventional MHC-I glycoproteins are widely expressed membrane-bound heterodimers consisting of a highly polymorphic MHC-encoded heavy chain noncovalently complexed with the β_2-microglobulin (β_2m) light chain (1). They present cytosol-derived short peptide antigens to the $\alpha\beta$ T cell receptor of $CD8^+$ cytotoxic T cells, thereby initiating the cell-mediated immune response (2). In humans there are three such genes, HLA-A, HLA-B, and HLA-C, also referred to as classical MHC-I. Similar to this first group is another trio, namely HLA-E, HLA-F, and HLA-G, dubbed nonclassical given their narrow pattern of tissue expression and especially their failure to participate in the canonical $\alpha\beta$ T cell receptor interaction (3). Instead, they are recognized by a heterogeneous family of immunoreceptors including γδ T cell receptor, NK, T, and myeloid Ig and/or lectin-like inhibitory and activatory receptors (4). Despite this profound functional dichotomy, the HLA-A–G belong to the same structural lineage, as they collectively share over 70% amino acid identity. In this context, the identification of a second lineage of class I genes within the MHC per se was unexpected and intriguing. These MHC class I chain-related *MIC* genes are remote members of the extended MHC-I superfamily, with seven members scattered throughout the entire 1.8-Mb MHC class I region (5, 6). Within this family, the closely linked *MICA* and *MICB* loci are juxtaposed to the *HLA-B* locus on the centromeric end of the complex and encode single-chain (non β_2m-linked), stress-induced, mucosa-specific class I-like glycoproteins that have been shown to interact with the gut-enriched Vδ1-bearing γδ T cells and/or T and NK cells coexpressing the C-type lectin NKG2D activating receptor (7–9). The induction of MIC upon microbial/tumoral challenge defines a stress beacon potentially relevant for triggering the innate arm of the immune system (10, 11).

The clear distinction between classical and nonclassical loci is, however, first and foremost genetic (12). Whereas classical genes are highly polymorphic, nonclassical loci are almost invariable. Surprising, therefore, was the identification of a large allelic repertoire in the MICA and MICB loci. Sequence analysis of MICA in not more than a few hundred chromosomes unveiled the existence of 54 alleles, among which 47 encode distinct putative glycoproteins (6, 13–15). A much less thorough analysis of MICB diversity has uncovered 16 alleles (6, 16, 17). While unraveling this rich allelic repertoire, we came across a polymorphic short-tandem repeat sequence within the MICA transmembrane segment encoding various numbers of alanine residues with repetitions of the $(GCT)_n$ codon, where $n = 4, 5, 6, 9$, or 10, with an additional allele, 5.1, characterized by a guanine insertion after the second GCT triplet (18). The latter is the origin of a frame shift mutation leading to the occurrence of a premature stop codon within the transmembrane segment, which chops off the 42-aa-long MICA cytoplasmic tail. Interestingly, several population-wide allelotyping analyses have reported that this MICA008/5.1 allele (008 refers to the extracellular sequence) is indeed the most frequent MICA allele in several populations of distinct ethnical backgrounds, e.g., over half of Caucasians carry this allele (14, 19, 20).

Cytoplasmic tail sequences are known to carry organelle-specific retention sequences or subcellular sorting motifs relevant for optimal functional behavior of a number of proteins (21, 22). Given the apparent localization of MICA in the intestinal epithelium, which serves as a paradigm for cellular polarity, the existence of such putative sequences within the cytoplasmic tail of the molecule seemed plausible. The intestinal epithelium is composed of a sheet of polarized epithelial cells, collectively the largest bodily interface with the environment (23). The plasma membrane of these cells is separated by tight junctions into apical (or luminal) and basolateral domains with distinct functional characteristics. The latter define the prime contact surface with the large number of the intraepithelial T and NK lymphocytes (IELs) shielding the entire gut surface against microbial or tumor invasion attempts (24). In the human small intestine and colon for instance, γδ T cells make up to 5–15% and 40% of IELs, respectively (25). However, our knowledge of the intracellular trafficking of MICA is nil. Intrigued by the identification of the peculiar MICA008/5.1 allele and its relatively high prevalence in the population, we set to analyze the functional

IMMUNOLOGY

Abbreviations: IELs, intraepithelial T and NK lymphocytes; MDCK, Madin–Darby canine kidney; GFP, green fluorescent protein; HRP, horseradish peroxidase.

¶To whom reprint requests should be addressed. E-mail: siamak@hemato-ulp.u-strasbg.fr or hinoko@is.icc.u-tokai.ac.jp.

The publication costs of this article were defrayed in part by page charge payment. This article must therefore be hereby marked "*advertisement*" in accordance with 18 U.S.C. §1734 solely to indicate this fact.

consequences of loosing the cytoplasmic tail, known in some cases to harbor sorting motifs. To do so, we constructed various native as well as cytoplasmic tail-deleted MICA-green fluorescent protein (GFP) expression constructs and visualized the subcellular localization of the molecule in polarized Madin–Darby canine kidney (MDCK) epithelial cells by confocal microscopy. Furthermore, we analyzed the expression of native MICA in its natural setting, human intestinal epithelium by using newly generated anti-MICA antibodies. Finally, by site-directed mutagenesis, we define the targeting motif responsible for this subcellular localization.

Materials and Methods

Expression Vectors. Human MICA cDNA clones with TM allele A5 were subcloned into the *Nhe*I/*Sma*I sites of the pEGFPN1 vector (pEGFP-MICA) (CLONTECH). The mutant MICA plasmid lacking the C-terminal 47 (pEGFP-MICAdel) residues was generated by ligating the N-terminal *Nhe*I--*Pvu*II fragment from human MICA cDNA with TM allele A5 to the *Nhe*I/*Sma*I sites of the pEGFPN1 vector. Both constructs therefore express the reporter protein in fusion to the C terminus of MICA. Native MICA (TM alleles A5 and A5.1) expression constructs were generated in the pCAGGS vector (pCAGGS-MICA and pCAGGS-MICA-A5.1) (26). Site-directed mutagenesis was done by using the QuickChange site-directed mutagenesis kit (Stratagene). The orientation and the nucleotide sequence of each construct was verified by DNA sequencing.

Cell Cultures and Transfections. MDCK cells were stably transfected with Lipofection reagent (DOTAP, Roche Molecular Biochemicals) by using 5 μg of pEGFP-MICA or pEGFPN1 according to the manufacturer's protocol and selected with 500 μg/ml of G418 (GIBCO/BRL) and screened for GFP fluorescence. Transient expression of the same cells with pEGFP-MICAdel, pCAGGS-MICA, and pCAGGS-MICA-A5.1 as well as amino acid substituted mutants were performed by using calcium phosphate (ProFection Mammalian Transfection Systems, Promega) following the manufacturer's instructions. Mouse myeloma (NS1) was transfected with 1 μg of pKJ2 (neomycin resistance gene) (27) and 5 μg of pCAGGS-MICA by using DOTAP lipofection reagent (Roche Molecular Biochemicals). Stable transfectants were selected in the presence of 500 μg/ml G418 (GIBCO/BRL) and cloned by limiting dilution.

Preparation of Anti-MICA Mouse Serum. The G418-resistant NS1 clones were screened for the expression of the transferred MICA gene by reverse transcriptase–PCR and Northern blot analysis. BALB/c mice (CLEA Japan, Osaka2) were injected i.p. five times at weekly intervals with paraformaldehyde-fixed NS1 cells expressing MICA mRNA. Sera were collected 5 weeks after the first immunization.

Cell-Surface Domain Selective Biotinylation Assay. The method described by Rosenthal and coworkers was slightly modified (28). Transwell polycarbonate filter-grown MDCK cells stably or transiently expressing GFP-tagged MICA molecules were labeled apically or basolaterally with EZ-Link Sulfo-NHS-LC-Biotin (Pierce). Biotinylated cell-surface proteins were labeled with anti-GFP rabbit (Molecular Probes) and anti-MICA mouse sera and then immunoprecipitated. Pellets were solubilized in Laemmli buffer, separated on SDS/PAGE (10% acrylamide), and blotted onto nitrocellulose membrane filters. Biotinylated proteins were detected by using horseradish peroxidase (HRP)-conjugated streptavidin (Amersham Pharmacia) and visualized with DAB (0.2 mg/ml 3,3'-diaminobenzidine, tetrahydrochloride/0.05 M Tris·HCl, pH 7.6/0.005% H_2O_2).

SDS/PAGE and Immunoblotting. Cell lysates were separated on 10% SDS/PAGE and transferred to nitrocellulose filters. Filters were incubated with either anti-MICA mouse serum or anti-GFP rabbit serum followed by anti-mouse or anti-rabbit HRP-conjugated secondary antibody (Amersham Pharmacia). Blots were developed by DAB or enhanced chemiluminescence (Amersham Pharmacia) by using Hyperfilm ECL (Amersham Pharmacia).

Confocal Microscopy. Transwell permeable filter-grown pEGFP-MICA and/or pEGFP-MICAdel-transfected MDCK cells were stained with Hoechst 33258 (Sigma) to visualize the nuclei. For the detection of MICA-A5.1 molecules, pCAGGS-MICA-A5.1-transfected polarized MDCK cells were apically surface labeled with biotin, incubated first with anti-MICA mouse serum, and then with FITC-conjugated sheep anti-mouse Ig and Texas Red-conjugated streptavidin (both from Amersham Pharmacia) and counterstained with Hoechst 33258. Filters were excised and transferred with the cell side up to a slide. Images were acquired by using a Zeiss Axioskop microscope equipped with a laser-scanning confocal unit (LSM-410, Carl Zeiss, Jena, Germany). GFP and/or FITC fluorescence and Texas Red fluorescence were excited by using the 488-nm Argon and 543-nm Helium Neon laser line and collected by using a dichroic beam splitter (NT 80/20/543, Zeiss) with emission filters, BP510–525 (Zeiss) and LP570 (Zeiss), respectively. Fluorescence associated with Hoechst 33258 was simultaneously excited by using the 351/364-nm Argon laser line and collected by using a dichroic beam splitter (NT 80/20/543, Zeiss) with an emission filter, LP397 (Zeiss). Three-dimensional reconstructions used the LSM software version 3.98 (Zeiss). Acquired images were imported into the Adobe PHOTOSHOP 5.0 for processing.

Immunofluorescence and Immunoelectron Microscopy. Tissue samples from surgical specimens were fixed overnight at 4°C with 4% paraformaldehyde/0.1 M sodium phosphate buffer and embedded in Tissue-Tek OCT compound (Sakura Fine Technical). Six-micromolar Cryostat sections were mounted on saline-coated slides and air dried, incubated with anti-MICA mouse serum and rabbit anti-alkaline phosphatase antibody, and revealed by using FITC-conjugated sheep anti-mouse Ig and Texas Red-conjugated donkey anti-rabbit Ig (Amersham Pharmacia). Sections with coverslips were examined by an Olympus fluorescence microscope. For immunoelectron microscopy, cryostat sections were labeled with anti-MICA mouse serum, followed by anti-mouse HRP-conjugated secondary antibody and stained with DAB solution. The preparations were postfixed in 2% osmic acid at room temperature for 1 h, dehydrated in a graded ethanol series, and embedded in Epon 812, according to the standard inverted gelatin capsule method. Ultrathin sections were prepared on an LKB ultramicrotome and observed with a JEOL 1200 EX electron microscope without counterstaining. As a negative control, the primary antibody was replaced by non-immune mouse serum.

Results and Discussion

MICA is the key member of a novel family of MHC-encoded class I-related loci involved in mucosal immunity (6). The expression of MICA and possibly MICB in the human gut foretold a putative strategic role for these molecules as a first line of defense in signaling stressed (infected, transformed) epithelial cells to neighboring NK and $\gamma\delta$ lymphocytes, the so called intraepithelial lymphocytes. This is corroborated by their augmented cell-surface expression during viral and bacterial infections as well as in tumors. Given the close contact of IELs with the basal and basolateral surfaces of enterocytes, it was of interest to investigate whether MICA was selectively routed to this location and, if so, to identify the nature and location of the

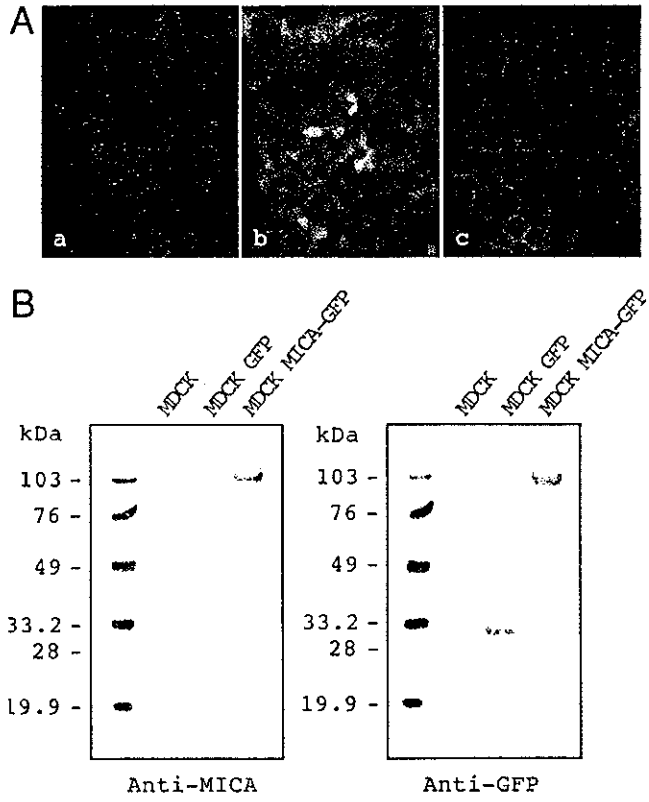

Fig. 1. Expression of GFP-tagged MICA molecules in MDCK cells. (*A*) Green fluorescence signals were detected by using fluorescence microscopy in MDCK cells that were nontransfected (*Left*), stably transfected with the control GFP (*Center*), or MICA-GFP expression plasmids (*Right*). (*B*) Immunoblot analysis of GFP-tagged MICA molecules in MDCK cells: nontransfected MDCK cells (Control), MDCK cell lines stably expressing GFP (GFP), and MICA-GFP. Transferred membrane was stained with anti-MICA mouse serum (*Left*) or anti-GFP rabbit serum (*Right*). Protein size markers (kDa) are shown on the left.

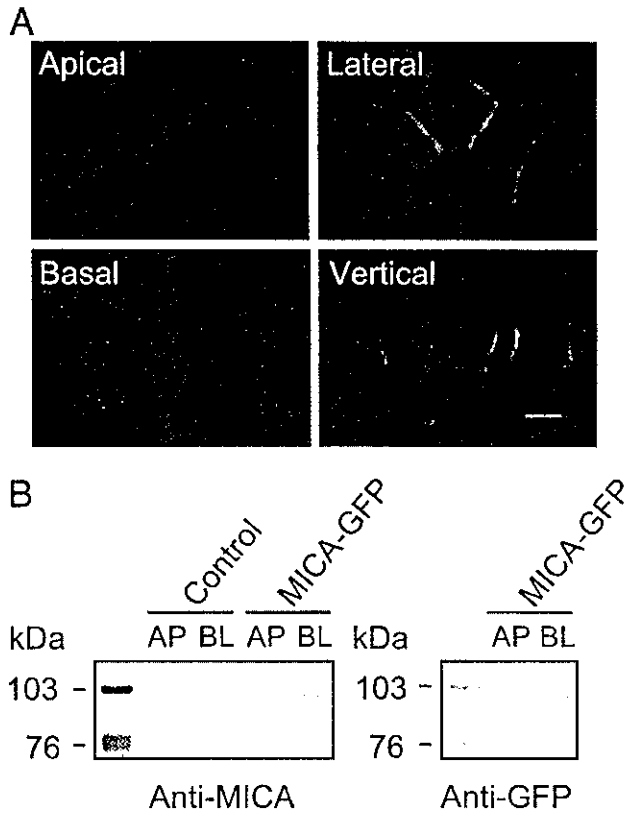

Fig. 2. Intracellular localization of GFP-tagged MICA molecules in polarized MDCK cells. (*A*) MDCK cells stably expressing GFP-tagged MICA molecules. MICA-GFP fluorescence is colored by green, and nuclei are colored by blue. Fluorescence signals were analyzed by laser-scanning confocal microscopy. Confocal fluorescence micrographs (*x–y* plane) were acquired at the apical (*Upper Left*), lateral (*Upper Right*), and basal region (*Lower Left*). Confocal fluorescence micrographs (*x–z* plane) showing the distribution of MICA-GFP along the apical-basal axis (vertical). The scale bar is 5 μm. (*B*) Domain-selective cell-surface biotinylation assay of MDCK cells. Stably transfected MDCK cells expressing GFP-tagged MICA molecules were biotinylated from either the apical (AP) or basolateral (BL) domain. Biotinylated proteins were recovered by immunoprecipitation with anti-MICA mouse serum (*Left*) or anti-GFP rabbit serum (*Right*) and detected by SDS/PAGE-immunoblot analysis by using HRP-conjugated streptavidin. Control lanes on the left panel correspond to untransfected cells. Protein size markers (kDa) are shown on the left.

sorting motif in the molecule. Given precedents having defined sorting signals in the cytoplasmic tails of other polarized molecules, we concentrated our attention on the MICA cytoplasmic tail and took advantage of the existence of a natural mutant that lacks this tail. Further impetus for our attention to this allele was its high frequency within several populations surveyed to date. To experimentally mimic the *in vivo* situation in the human gut, we carried out our studies in the MDCK system, widely used as a prototype for epithelial polarity (22, 29).

Expression and Intracellular Localization of GFP-Tagged MICA Molecules in MDCK Epithelial Cells. We first established an MDCK epithelial cell line stably expressing a GFP-tagged MICA (pEGFP-MICA) protein and traced GFP fluorescence to investigate the intracellular localization of MICA. Untransfected MDCK cells used as a negative control revealed no fluorescence signals, and cells transfected with the GFP expression plasmid (pEGFPN1) used as positive control revealed fluorescence evenly distributed throughout the intracellular compartments (Fig. 1*A Left* and *Center*). However, intense fluorescence of the MICA-GFP fusion proteins was clearly found at the plasma membrane (Fig. 1*A Right*). Fig. 1*B* shows immunoblot analysis of the same MDCK cells by using anti-MICA and anti-GFP sera. Immunoreactive proteins were recognized as a single 95-kDa band in MDCK cells stably expressing MICA-GFP fusion molecules, by using either anti-MICA mouse serum (*Left*) or anti-GFP rabbit serum (*Right*). Anti-MICA mouse serum raised in this report reacted specifically with a protein of 65 kDa in pCAGGS-MICA-transfected NS1 cells but did not detect any bands in untransfected NS1 cells, pCAGGS-MICB NS1 cells, or pEGFP-MICB MDCK cells (data not shown). Finally and as shown in the Fig. 1*B Right*, GFP expression alone yielded the expected 30-kDa single band as evidenced by using anti-GFP rabbit serum.

Subcellular routing of MICA was analyzed by laser-scanning confocal microscopy in monolayers of MDCK cells stably expressing GFP-tagged MICA molecules. *En face* images reveal a honeycomb pattern of GFP signals (Fig. 2*A Upper Right*), whereas the vertical scan confirms an almost exclusive basolateral localization of the GFP-tagged MICA (Fig. 2*A Lower Right*) (with apparently more protein at the lateral with respect to the basal surface).

To confirm the steady-state distribution of GFP-tagged MICA, a domain-selective cell-surface biotinylation assay in which transfected MDCK monolayers were selectively biotinylated from either surface was carried out. In agreement with confocal results, the majority of GFP-tagged MICA molecules were found to be expressed basolaterally with an apparent molecular mass of 95 kDa (Fig. 2*B*). The tightness of the

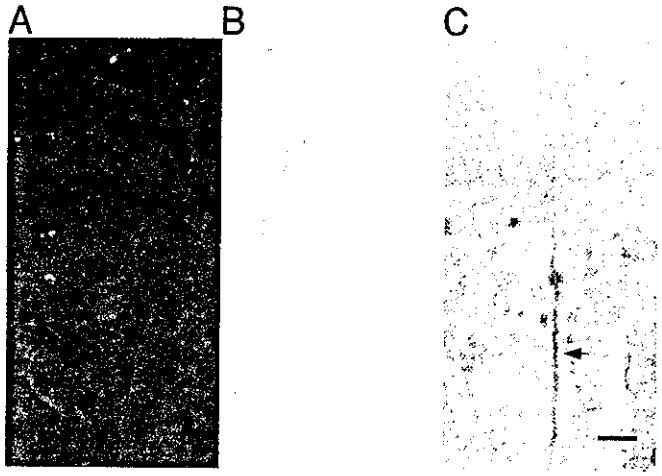

Fig. 3. Immunofluorescence and immunoelectron micrographs of human intestinal epithelium sections stained with anti-MICA mouse serum. (*A*) Human intestinal epithelium was double-stained with anti-MICA mouse serum and FITC-conjugated anti-mouse Ig (green) and anti-intestinal alkaline phosphatase rabbit serum and Texas Red-conjugated anti-rabbit Ig (red). (*B*) Immunohistochemical detection of MICA in human intestinal epithelium by staining with anti-MICA mouse serum and HRP-conjugated anti-mouse Ig. (*C*) The ultrastructural localization of MICA molecules in human intestinal epithelial cells was analyzed by immunoelectron microscope employing anti-MICA mouse serum and HRP-conjugated secondary antibody. (Scale bar = 500 nm.)

epithelial monolayers used in these experiments was verified by quantification of biotin leakage to the opposite side of the filters (30), which was found to be less than 0.2% over 3 days (data not shown).

MICA Is Expressed at the Basolateral Surface of the Human Intestinal Epithelial Cells. As described above, we showed that human GFP-tagged MICA is located at the basolateral plasma membrane of stably transfected canine polarized epithelial cells. Because it is not known whether MICA molecules are similarly polarized to the basolateral plasma membrane of human enterocytes, we visualized the intracellular localization of MICA in human intestine by using immunofluorescence and immunohistochemistry. Double labeling of cryosections of the human intestinal epithelium with anti-MICA and anti-intestinal alkaline phosphatase sera depicts a nonoverlapping fluorescent pattern establishing distinctive cellular distribution for these molecules. Whereas anti-intestinal alkaline phosphatase is well known to specifically label the apical membrane, the anti-MICA staining establishes a basal as well as lateral expression pattern (Fig. 3*A*). Similarly, immunoperoxidase staining by using the anti-MICA mouse serum revealed MICA expression at the basolateral plasma membrane of intestinal epithelium (Fig. 3*B*). This was further confirmed, at high resolution, by immunoelectron microscopy, which revealed an identical subcellular localization for MICA (Fig. 3*C*). A similar staining pattern was observed in human epithelial cells isolated from different individuals (data not shown).

Dihydrophobic Amino Acids Leu-Val at Codons 344–345 of the MICA Cytoplasmic Tail Are Required for Basolateral Sorting. Efficient basolateral sorting of some transmembrane proteins has been reported to depend on a sorting signal within their cytoplasmic domains (22). To test whether the cytoplasmic tail of MICA contains such a signal, C-terminally truncated MICA cDNA lacking the entire cytoplasmic domain plus 5 aa of the transmembrane domain (47 aa in total) was fused to a GFP reporter

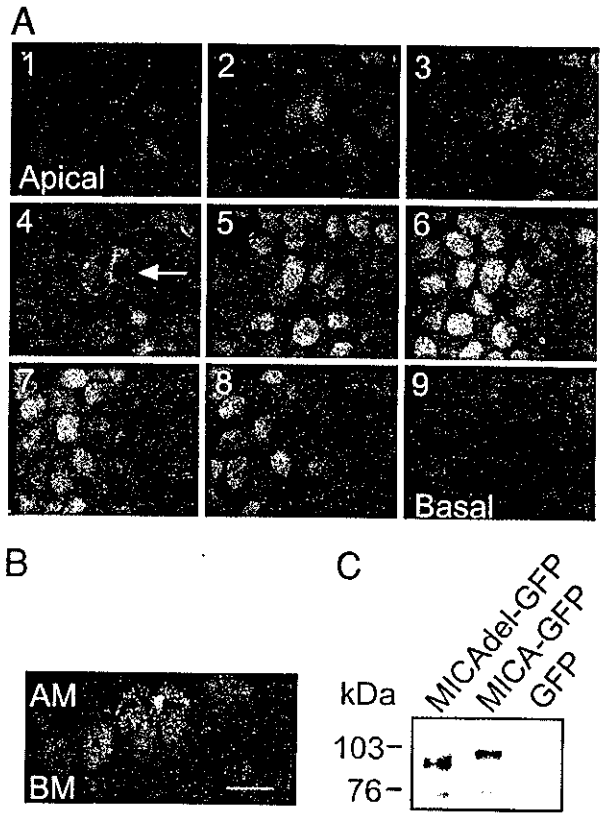

Fig. 4. Intracellular localization of GFP-tagged MICA mutant molecules lacking the cytoplasmic domain in polarized MDCK cells. (*A*) MDCK cells were transiently transfected with the pEGFP-MICAdel plasmid (which lacks the 47 residues C terminus of the protein). Confocal fluorescence micrographs (*x–y* plane), beginning at the apical membrane (section 1, *Upper Left*) and ending at the basal membrane (section 9, *Lower Right*) were acquired in 1.0-μm increments. Arrow in optical section 4 indicates the plane of vertical section. (*B*) Confocal fluorescence micrograph (*x–z* plane) shows the distribution of GFP-tagged MICA mutant molecules lacking the cytoplasmic domain along the apical–basal axis. GFP-tagged mutant MICA-derived fluorescence is colored by green and nuclei by blue. AM, apical membrane; BM, basal membrane. The scale bar is 10 μm. (*C*) Immunoblot analysis of transiently expressed GFP-tagged mutant MICA molecules in MDCK cells. MDCK cells, transiently transfected with the pEGFP-MICA (MICA-GFP) or with pEGFP-MICAdel (MICAdel-GFP) plasmids, were immunoblotted with anti-MICA mouse serum. A control consisted of MDCK cells stably expressing GFP molecules alone. Sizes of marker proteins used in kDa are shown on the left.

gene and transiently expressed in MDCK cells. The hybrid glycoprotein had an expected molecular mass of 91 kDa (roughly 5 kDa smaller than the 95 kDa for full-length MICA-GFP fusion protein) as revealed by both anti-MICA (Fig. 4*C*) and anti-GFP sera (data not shown). Confocal laser-scanning microscopy clearly indicated that C-terminally truncated MICA-GFP molecule was predominantly localized to the apical side of the cell (whether this apical staining represents cell-surface expression on the plasma membrane and/or reflects the localization of the mutant protein in as yet to be identified intracellular storage/transit compartment remains an open question), as opposed to basolateral targeting for native MICA (Fig. 4 *A* and *B*). This result suggests that the C-terminal 47-aa residues of MICA contain the necessary information required for this basolateral targeting.

Cytoplasmic tail dihydrophobic sequences have been shown to be responsible for subcellular sorting of CD44 in MDCK cells (31). There are three such dihydrophobic pairs in the cytoplasmic tail of MICA (numbering according to that in A5 allele):

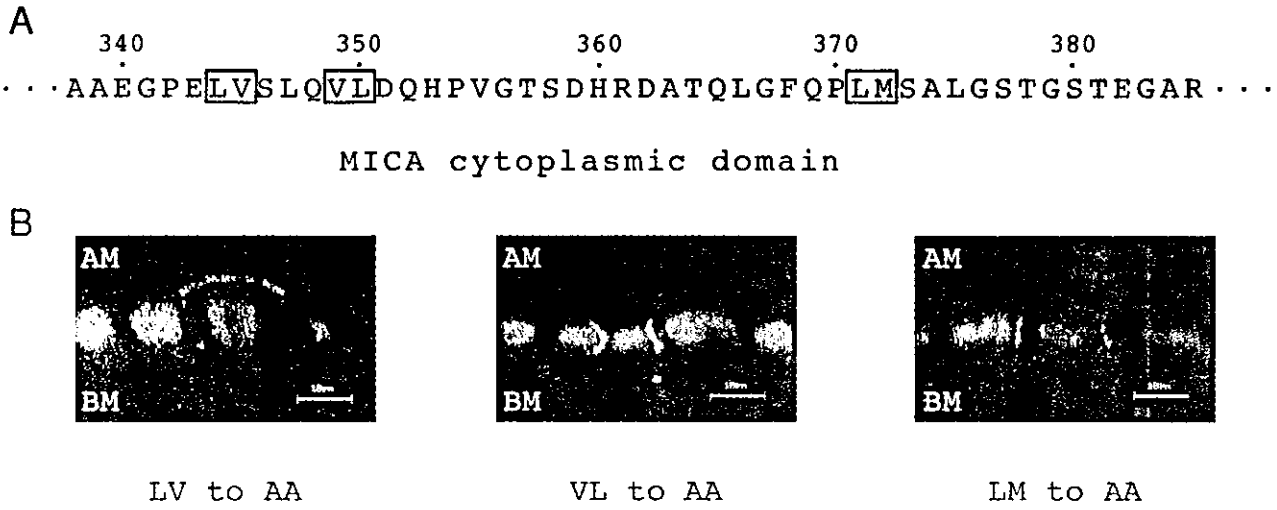

Fig. 5. Determination of the basolateral sorting motif within the MICA cytoplasmic domain by alanine substitution analysis. (*A*) The MICA cytoplasmic tail sequence. Boxes highlight dihydrophobic amino acids that were substituted by Ala-Ala via site-directed mutagenesis. (*B*) MDCK cells were transiently transfected with the alanine-substituted pEGFP-MICA plasmids. Confocal fluorescence micrographs were acquired in 1.0-μm increments. Confocal fluorescence images showing the distribution of alanine-substituted GFP-tagged MICA molecules along the apical-basal axis. GFP-tagged MICA-derived fluorescence is colored by green and nuclei by blue. AM, apical membrane; BM, basal membrane. (Scale bar = 10 μm.)

Leu-Val (344–345), Val-Leu (349–350), and Leu-Met (371–372). These pairs were sequentially changed to Ala-Ala by site-directed mutagenesis of the pEGFP-MICA plasmid and transfected back into MDCK cells (Fig. 5*A*). Although mutagenesis of the last two pairs did not affect the subcellular localization of the recombinant molecule, that of the first pair, Leu-Val (344–345), shifted the MICA localization from basolateral to apical, defining hence this discrete sequence as the MICA basolateral targeting sequence (Fig. 5*B*).

The A5.1 Frame Shift Mutation in the MICA Transmembrane Domain Creates a Presumably Defective Allele Resulting in a Loss of Basolateral Targeting. A triplet repeat short-tandem repeat polymorphism was previously identified in the transmembrane region of MICA, and six distinct alleles of this microsatellite were reported (18, 32). These are defined by (GCT = Alanine)$_{4,5,6,9,10}$ and one allele, A5.1, containing an additional one-base insertion (after the second GCT). The latter creates a frame shift mutation resulting in a premature termination codon within the transmembrane region itself, thus denying the molecule the sorting signal identified within the cytoplasmic domain. However, this particular allele has been frequently observed in all population studies carried out thus far, with the high gene frequencies up to 55% in Caucasians (14, 19, 20). To confirm that this prevalent allele loses the ability to be targeted to the basolateral surface, MDCK cells were transiently transfected with MICA-A5.1 expression vector (pCAGGS-MICA-A5.1) and intracellular routing of the molecule traced. Transfected MDCK monolayers, in which the apical membrane was labeled with biotin, were fixed, permeabilized, and incubated with anti-MICA mouse serum on both the apical and basolateral sides. These cells were then stained with a sheep anti-mouse FITC-conjugated secondary antibody and Texas Red-conjugated streptavidin. Confocal laser-scanning microscopy analysis revealed that MICA-A5.1 molecules were predominantly localized to the apical plasma membrane region in fully polarized MDCK cells cultured on permeable filter supports. This finding was confirmed by double-labeling experiments by using polarized MDCK cells. After domain-selective cell-surface biotinylation to label the apical membrane, FITC signals marking the localization of MICA-A5.1 molecules were found to be colocalized with Texas Red signals derived from the biotin-labeled apical surface membrane (Fig. 6 *A* and *B*). On the other hand, FITC fluorescent signals in MDCK cells transfected with the pCAGGS-MICA plasmid expressing the MICA A5 allele were predominantly localized to the basolateral plasma membrane (Fig. 6*C*). Thus, these data establish that MICA-A5.1 moves to an apparently incorrect destination, i.e., apical plasma membrane in contrast to the basolateral localization of the A5 and presumably all other alleles.

In summary, we report the identification of a dihydrophobic Leu-Val tandem sequence in the cytoplasmic tail of MICA responsible for targeting the protein to the basolateral plasma membrane of the gut epithelial cells, the prime site of contact with the effector NK and T IELs. Thus, the incorrect membrane

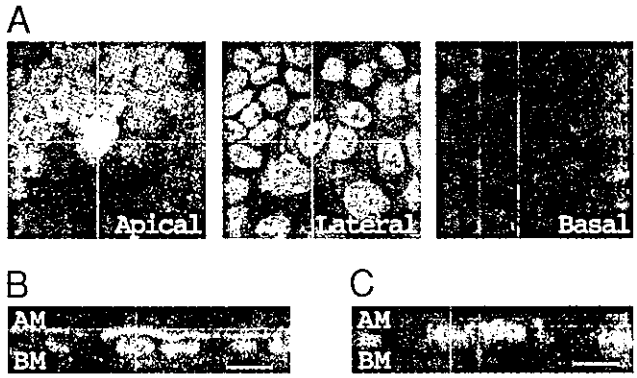

Fig. 6. Intracellular localization of MICA-A5.1 molecules in polarized MDCK cells. (*A*) MDCK cells were transiently transfected with the pCAGGS-MICA-A5.1 plasmid. Monolayers were labeled for the apical membrane with biotin and then washed, fixed, and stained with anti-MICA mouse serum and FITC-conjugated secondary antibody. The apical cell-surface membrane was visualized by Texas Red-conjugated streptavidin. Fluorescence of MICA-A5.1 is colored by green and the apical plasma membrane by red. The fluorescence signals were analyzed by laser-scanning confocal microscopy. Confocal fluorescence micrographs (*x–y* plane) were acquired at the apical (*Left*), lateral (*Center*), and basal (*Right*) regions. (*B*) Confocal fluorescence micrographs (*x–z* plane) showing the distribution of MICA-A5.1 along the apical-basal axis. (*C*) MDCK cells were transiently transfected with pCAGGS-MICA and stained with anti-MICA mouse serum and FITC-conjugated secondary antibody. Nuclei stained with Hoechst 33258 are colored in blue. AM, apical membrane; BM, basal membrane. (Scale bar = 10 μm.)

localization of MICA-A5.1 is plausibly associated with functional deficiency, and A5.1 homozygous individuals are possibly defective in immune surveillance exerted by intestinal IELs against various epithelial malignancies as recently corroborated by the demonstration of an analogous function for the NKG2D-interacting RAE1/H60 loci, murine functional homologs of MIC genes (33–35).

We thank Dr. Johbu Ito and Mr. Akira Akatsuka for technical help in confocal microscopy, and Dr. Masataka Kuwana for providing the MICA-A5.1 cDNA clone. S.B. acknowledges financial support from the Institut National de la Santé et de la Recherche Médicale-Contrat de Recherche Stratégique and the Actions Concertées Incitatives Jeunes Chercheurs and Biologie du Développement et Physiologie Intégrative-Ministère de la Recherche.

1. Madden, D. R. (1995) *Annu. Rev. Immunol.* **13,** 587–622.
2. Rock, K. L. & Goldberg, A. L. (1999) *Annu. Rev. Immunol.* **17,** 739–779.
3. Maenaka, K. & Jones, E. Y. (1999) *Curr. Opin. Struct. Biol.* **9,** 745–753.
4. Lanier, L. L. (1998) *Cell* **92,** 705–707.
5. Bahram, S., Bresnahan, M., Geraghty, D. E. & Spies, T. (1994) *Proc. Natl. Acad. Sci. USA* **91,** 6259–6263.
6. Bahram, S. (2000) *Adv. Immunol.* **76,** 1–60.
7. Groh, V., Steinle, A., Bauer, S. & Spies, T. (1998) *Science* **279,** 1737–1740.
8. Bauer, S., Groh, V., Wu, J., Steinle, A., Phillips, J. H., Lanier, L. L. & Spies, T. (1999) *Science* **285,** 727–729.
9. Wu, J., Song, Y., Bakker, A. B., Bauer, S., Spies, T., Lanier, L. L. & Phillips, J. H. (1999) *Science* **285,** 730–732.
10. Groh, V., Rhinehart, R., Randolph-Habecker, J., Topp, M. S., Riddell, S. R. & Spies, T. (2001) *Nat. Immunol.* **2,** 255–260.
11. Das, H., Groh, V., Kuijl, C., Sugita, M., Morita, C. T., Spies, T. & Bukowski, J. F. (2001) *Immunity* **15,** 83–93.
12. Parham, P. & Ohta, T. (1996) *Science* **272,** 67–74.
13. Fodil, N., Laloux, L., Wanner, V., Pellet, P., Hauptmann, G., Mizuki, N., Inoko, H., Spies, T., Theodorou, I. & Bahram, S. (1996) *Immunogenetics* **44,** 351–357.
14. Fodil, N., Pellet, P., Laloux, L., Hauptmann, G., Theodorou, I. & Bahram, S. (1999) *Immunogenetics* **49,** 557–560.
15. Robinson, J., Perez-Rodriguez, M., Waller, M. J., Cuillerier, B., Bahram, S., Yao, Z., Albert, E. D., Madrigal, J. A. & Marsh, S. G. (2001) *Immunogenetics* **53,** 150–169.
16. Pellet, P., Renaud, M., Fodil, N., Laloux, L., Inoko, H., Hauptmann, G., Debre, P., Bahram, S. & Theodorou, I. (1997) *Immunogenetics* **46,** 434–436.
17. Ando, H., Mizuki, N., Ota, M., Yamazaki, M., Ohno, S., Goto, K., Miyata, Y., Wakisaka, K., Bahram, S. & Inoko, H. (1997) *Immunogenetics* **46,** 499–508.
18. Mizuki, N., Ota, M., Kimura, M., Ohno, S., Ando, H., Katsuyama, Y., Yamazaki, M., Watanabe, K., Goto, K., Nakamura, S., *et al.* (1997) *Proc. Natl. Acad. Sci. USA* **94,** 1298–1303.
19. Petersdorf, E. W., Shuler, K. B., Longton, G. M., Spies, T. & Hansen, J. A. (1999) *Immunogenetics* **49,** 605–612.
20. Fischer, G., Arguello, J. R., Perez-Rodriguez, M., McWhinnie, A., Marsh, S. G., Travers, P. J. & Madrigal, J. A. (2000) *Immunogenetics* **51,** 591–599.
21. Pelham, H. R. (1999) *Philos. Trans. R. Soc. London B* **354,** 1471–1478.
22. Mostov, K. E., Verges, M. & Altschuler, Y. (2000) *Curr. Opin. Cell Biol.* **12,** 483–490.
23. Shao, L., Serrano, D. & Mayer, L. (2001) *Semin. Immunol.* **13,** 163–176.
24. Lefrancois, L., Fuller, B., Huleatt, J. W., Olson, S. & Puddington, L. (1997) *Springer Semin. Immunopathol.* **18,** 463–475.
25. Kagnoff, M. F. (1998) *Am. J. Physiol.* **274,** G455–G458.
26. Niwa, H., Yamamura, K. & Miyazaki, J. (1991) *Gene* **108,** 193–199.
27. Boer, P. H., Potten, H., Adra, C. N., Jardine, K., Mullhofer, G. & McBurney, M. W. (1990) *Biochem. Genet.* **28,** 299–308.
28. Schulein, R., Lorenz, D., Oksche, A., Wiesner, B., Hermosilla, R., Ebert, J. & Rosenthal, W. (1998) *FEBS Lett.* **441,** 170–176.
29. Ikonen, E. & Simons, K. (1998) *Semin. Cell Dev. Biol.* **9,** 503–509.
30. Hershberg, R. M., Cho, D. H., Youakim, A., Bradley, M. B., Lee, J. S., Framson, P. E. & Nepom, G. T. (1998) *J. Clin. Invest.* **102,** 792–803.
31. Sheikh, H. & Isacke, C. M. (1996) *J. Biol. Chem.* **271,** 12185–12190.
32. Perez-Rodriguez, M., Corell, A., Arguello, J. R., Cox, S. T., McWhinnie, A., Marsh, S. G. E. & Madrigal, J. A. (2000) *Tissue Antigens* **55,** 162–165.
33. Diefenbach, A., Jensen, E. R., Jamieson, A. M. & Raulet, D. H. (2001) *Nature (London)* **413,** 165–171.
34. Cerwenka, A., Baron, J. L. & Lanier, L. L. (2001) *Proc. Natl. Acad. Sci. USA* **98,** 11521–11526.
35. Girardi, M., Oppenheim, D. E., Steele, C. R., Lewis, J. M., Glusac, E., Filler, R., Hobby, P., Sutton, B., Tigelaar, R. E. & Hayday, A. C. (2001) *Science* **294,** 605–609.

Male-specific suppression of hepatic microsomal UDP-glucuronosyltransferase activities toward sex hormones in the adult male rat administered bisphenol A

Noriaki SHIBATA*, Junya MATSUMOTO*, Ken NAKADA†, Akira YUASA* and Hiroshi YOKOTA*[1]

*Department of Veterinary Biochemistry, Rakuno Gakuen University, Ebetsu, Hokkaido 069-8501, Japan, and †Department of Veterinary Obstetrics and Gynecology, School of Veterinary Medicine, Rakuno Gakuen University, Ebetsu, Hokkaido 069-8501, Japan

Various adverse effects of endocrine disruptors on the reproductive organs of male animals have been reported. We found that UDP-glucuronosyltransferase (UGT) activities towards bisphenol A, testosterone and oestradiol were significantly decreased in liver microsomes prepared from adult male Wistar rats administered with the endocrine disruptor bisphenol A (1 mg/2 days for 2 or 4 weeks). However, suppression of the transferase activities was not observed in female rats, even after bisphenol A treatment for 4 weeks. Diethylstilbestrol, which is well known as an endocrine disruptor, had the same effects, but *p*-cumylphenol had no effect on UGT activities towards sex hormones. Co-administration of an anti-oestrogen, tamoxifen, inhibited the suppression of the transferase activities by bisphenol A. Western blotting analysis showed that the amount of UGT2B1, an isoform of UGT which glucuronidates bisphenol A, was decreased in the rat liver microsomes by the treatment. Northern blotting analysis also indicated that UGT2B1 mRNA in the liver was decreased by bisphenol A treatment. The suppression of UGT activities, UGT2B1 protein and UGT2B1 mRNA expression did not occur in female rats. The results indicate that bisphenol A treatment reduces the mRNA expression of UGT2B1 and other UGT isoforms that mediate the glucuronidation of sex hormones in adult male rats, and this suggests that the endocrine balance may be disrupted by suppression of glucuronidation.

Key words: glucuronidation, oestradiol, xeno-oestrogen.

INTRODUCTION

There are many substances that are considered to be environmental oestrogens, including pesticides, pollutants and various chemicals [1]. Bisphenol A (BPA), which is widely used in the chemical industry in the manufacturing of epoxy, polycarbonate and polyester-styrene resins, and in dentistry [2], is regarded as an environmental oestrogen. BPA has been shown to act on MCF-7 human breast cancer cells as an oestrogen by stimulating cellular proliferation and inducing progesterone receptors [3]. BPA has also been shown to bind to oestrogen receptors, and the oestrogenic effects induced by BPA were blocked by the oestrogen antagonist tamoxifen, thus supporting the notion that the oestrogenic activity of BPA is mediated via the oestrogen receptor [3]. Recently, some adverse *in vivo* effects of BPA have been reported. Treatment with a single high dose of BPA (37.5–150 mg/kg) induced growth, differentiation and c-*fos* protooncogene expression in the female reproductive tract [4]. Despite the more than 100-fold lower binding affinities for the oestrogen receptors (ERα and ERβ) compared with β-oestradiol, a low dose of BPA exhibited adverse effects on reproductive organs. Prenatal treatment with BPA (2.4 mg/kg for 7 days in pregnant CF-1 mice) significantly reduced the number of days between vaginal opening and first vaginal oestrus in females, which located between two female fetuses [5]. Plasma free testosterone levels were dramatically decreased by treatment of mice with BPA (about 13 mg/day per kg body weight) for 8 weeks, and prepubertal and/or pubertal exposure to a environmental oestrogen specifically disrupted male reproductive functions in mice [6]. It has recently been reported that there were significant positive correlations between BPA exposure and serum testosterone concentrations in the subjects [7].

We recently reported that BPA was glucuronidated by an isoform of UDP-glucuronosyltransferase (UGT; EC 2.4.1.17), UGT2B1, in the rat liver [8], and that most of the chemical was then excreted into the bile as a glucuronide [9]. In the present study, oral administration of BPA (2 mg/kg per day for 2 or 4 weeks) was found to result in a decrease in UGT activities towards sex hormones and BPA in the liver of male, but not female, rats.

EXPERIMENTAL

Materials

Cholic acid, purchased from Nissui Yakuhin Co. (Tokyo, Japan), was further purified and converted to its sodium salt [10]. UDP-glucuronic acid was obtained from Nakarai Yakuhin Co. (Kyoto, Japan). *p*-Cumylphenol was from Wako Chemicals, Co. (Osaka, Japan). BPA, diethylstilbestrol (DES), DES-glucuronide, testosterone, oestradiol, oestradiol 17β-glucuronide and oestradiol 3α-glucuronide were obtained from Sigma Chemical Co. Nylon membrane (Hybond N$^+$) was obtained from Amersham, and Trizol™ reagent was obtained from Gibco BRL. Other reagents were of the highest grade available.

Administration of BPA to rats

Adult male and female Wistar rats (approx. 250 g, 9 weeks old) were used in this study. BPA (1 mg), DES (1 mg), *p*-cumylphenol

Abbreviations used: BPA, bisphenol A; DES, diethylstilbestrol; ER, oestrogen receptor; UGT, UDP-glucuronosyltransferase.

[1] To whom correspondence should be addressed (e-mail h-yokota@rakuno.ac.jp).